Surface plasmon resonance phase-shift interferometry: Real-time DNA microarray hybridization analysis

Shean-Jen Chen
Yuan-Deng Su
National Cheng Kung University
Department of Engineering Science
Tainan 701, Taiwan

Feng-Ming Hsiu
Chia-Yuan Tsou
Yi-Kuang Chen
National Central University
Department of Mechanical Engineering
Chung-Li 320, Taiwan

Abstract. Surface plasmon resonance (SPR) phase-shift interferometry (PSI) is a novel technique which combines SPR and modified Mach–Zehnder PSI to measure the spatial phase variation caused by biomolecular interactions upon a sensing chip. The SPR-PSI imaging system offers high resolution and high-throughout screening capabilities for microarray DNA hybridization without the need for additional labeling, and provides valuable quantitative information. The SPR-PSI imaging system has an enhanced detection limit of 2.5×10^{-7} refraction index change, a long-term phase stability of $\pi/100$ in 30 min, and a spatial phase resolution of $\pi/300$ with 100×100 μm^2 detection area. This study successfully demonstrates the label-free observation of 15-mer DNA microarray.
[DOI: 10.1117/1.1924713]

Keywords: surface plasmon resonance; imaging system; microarray; DNA hybridization; phase-shifting interferometry.

Paper 03020 received Feb. 26, 2004; revised manuscript received Aug. 23, 2004; accepted for publication Dec. 20, 2004; published online Jun. 1, 2005.

1 Introduction

The surface plasmon resonance (SPR) biosensor has developed into a valuable biomolecular detection technique since it is sensitive to even very small environmental changes and does not require the extrinsic labeling of the biomolecules of interest. Through the biospecific capturing of molecules immobilized on its surface, the SPR device provides the ability to detect biomaterial concentration, thickness, and binding kinetic data for specific biological analytes. A review of the related literature reveals that SPR systems have been applied in an ever increasing number of biomolecular interaction analysis applications since 1990, including antigen–antibody interactions, receptor–ligand interactions, DNA–protein interactions, and DNA hybridization.[1–3]

The SPR sensor is based on a coupling prism coated with a thin metal layer. Typically, the layer takes the form of a 50-nm-thick Au or Ag thin film, and serves to provide an optimum resonance condition in the near infrared and visible light regions. In an excitation method known as attenuated total reflection (ATR),[4] the surface plasmon wave (SPW), i.e., a charge density wave propagating along the interface between the metal layer and the dielectric medium, absorbs the energy of the evanescent wave from the incident *P*-wave light which would otherwise be totally reflected if the metal film was not present. Hence, the reflectivity of the incident light is decreased. The SPR phenomenon can be observed via an absorption spectrum in the dependence of the intensity of the *P*-wave light reflected from the metal film. Biosensing techniques generally employ one of two different interrogation modes, namely incident angular interrogation or wavelength interrogation. SPR sensors based on wavelength interrogation are less precise than those that apply angular interrogation due to the limited resolving power ($\lambda/\Delta\lambda$) of the optical spectrum analyzer. Nevertheless, when the resolving power exceeds 10^5 in the near infrared and visible light regions, wavelength interrogation is preferred since it permits a more compact optical system. In a SPR biosensor, biomolecular interaction at the sensing surface results in a detectable change in the refractive index or thickness of the biomolecular layer located on the biosensor surface. Angular interrogation enables the prompt detection of the corresponding resonant angular shift when the conditions of surface plasmon excitation are satisfied.[5,6] SPR biosensors are generally based on a prism-coupler ATR system, and operate in four principal detection approaches, namely intensity measurement, angular interrogation, wavelength interrogation, and phase measurement. It has been shown that the sensitivity of modern SPR sensing systems based on both the angular interrogation and phase measurement techniques is such that they are capable of detecting refractive indexes as high as approximately 5×10^{-7} refractive index units, which corresponds to a 1 pg/mm^2 surface coverage of biomolecules.[7]

Although the commercially successful ''BIAcore'' SPR system (BIAcore AB, Uppsala, Sweden) based on angular interrogation has been used previously to analyze biomolecular interactions, it does not possess an imaging capability (high-throughput screening).[8] Current trends concerning advanced SPR biosensors and systems not only include the improvement of their sensitivity, resolution, stability, and speed, but

Address all correspondence to Shean-Jen Chen. Tel.: +886-6-2757575 ext. 63351; Fax: +886-6-2766549; E-mail: sheanjen@mail.ncku.edu.tw

1083-3668/2005/$22.00 © 2005 SPIE

also the development of high-throughput screening capabilities. Achieving this screening capability and simultaneously retaining a detection limit of 1 pg/mm^2 requires the use of SPR microarrays and associated detection systems. In the conventional SPR imaging system, a collimated light source is used to illuminate a coupling prism or grating with a thin gold film sample assembly at an incident angle close to the SPR angle. The variation in the intensity of the reflected light is then detected at a fixed angle using an area scan charged-coupled device (CCD) camera, which subsequently produces the corresponding SPR image. Even though such SPR imaging systems are capable of high-throughput screening, they struggle to detect low concentrations of low molecular weight analytes.[9–12] A localized surface plasmon resonance biosensor based on colloidal gold nanoparticles sensitized with the binding protein can achieve the necessary high-throughput screening capability, but the detection capabilities of this particular biosensor are limited to an area mass detection limit of 100–1000 pg/mm^2, which is a factor of at least 100 times poorer than that of conventional SPR biosensors.[13,14] Several SPR interferometers have been developed to measure the spatial phase variation associated with SPR, but the systemic modular and integration and fringe analysis remain problematic.[15–18] Consequently, this study proposes a novel SPR imaging system based on modified Mach–Zehnder phase-shifting interferometry (PSI) in which the spatial phase variation of a resonantly reflected light is measured in order to observe DNA microarray hybridization. It is shown that the detection limit of the developed SPR-PSI imaging system is improved to approximately 2.5×10^{-7} refraction index change at each individual spot, which represents a resolution improvement of 1–2 orders compared to that of conventional SPR imaging systems.

2 Excitation of Surface Plasmon Resonance by Light

SPR is an optical phenomenon in which incident *P*-wave light excites a SPW such that it reaches a resonance condition. Excitation of the SPR occurs when the parallel component of the wave vectors of the incident light, k_x^l, and the wave vector of the SPW, k_{spw}, satisfy the following matching condition:[4]

$$k_x^l = k_0(\varepsilon_0)^{1/2}\sin\theta = k_{\mathrm{spw}}, \tag{1}$$

where θ is the incident angle of the light and ε_0 is the wavelength-dependent dielectric constant of the prism. The wave vector of the SPW can be approximated by

$$k_{\mathrm{spw}} \cong k_0\left(\frac{\varepsilon_1\varepsilon_2}{\varepsilon_1+\varepsilon_2}\right)^{1/2}, \tag{2}$$

where ε_2 and ε_1 are the wavelength-dependent complex dielectric constants of the dielectric sample and the metal, respectively.

When the matching condition of Eq. (1) is satisfied, most of the incident light energy is transferred to the surface plasmon, i.e., most of the incident light is absorbed by the excitation of SPW. This phenomenon results in an attenuated reflected spectrum.

Most common SPR sensors are based on the prism coupler-based SPR system (ATR) shown in Fig. 1. As can be seen, this configuration comprises of a prism, a thin metal film, and a dielectric layer in which the analytes of interest are immobilized. Theoretical results obtained using Fresnel's equations demonstrate that the reflectivity minimum (i.e., strong absorption) occurs only for the *P*-wave light. The nature of the reflection spectrum is determined by the molecular concentration and thickness of the biomaterials. The quantitative description of the reflectivity *R* for the *P* wave is given by Fresnel's equations for systems comprising three or more layers as

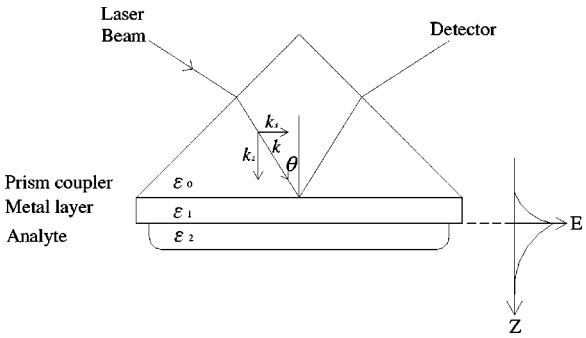

Fig. 1 Kretschmann configuration of SPR biosensors.

$$R \equiv |r_{012}^p|^2 = \left|\frac{r_{01}^p + r_{12}^p\exp(2ik_{z1}d)}{1 + r_{01}^p r_{12}^p\exp(2ik_{z1}d)}\right|^2, \tag{3}$$

where d is the thickness of the metal film, and the reflection coefficient of the *P* wave is given by

$$r_{ik}^p = \left(\frac{k_{zi}}{\varepsilon_i} - \frac{k_{zk}}{\varepsilon_k}\right) \Big/ \left(\frac{k_{zi}}{\varepsilon_i} + \frac{k_{zk}}{\varepsilon_k}\right). \tag{4}$$

Moreover, $r_{012}^p = \mathrm{Re}(r_{012}^p) + \mathrm{Im}(r_{012}^p)$. Hence, the phase of the reflected light can be expressed as

$$\phi = \tan^{-1}(r_{012}^p) = \tan^{-1}[\mathrm{Im}(r_{012}^p)/\mathrm{Re}(r_{012}^p)]. \tag{5}$$

Figure 2 presents the simulated reflectivity and phase shift curves of a SPR sensor with the following configuration: BK7 prism/ Au thin film/ biomaterial/ water buffer, with corresponding dielectric constants of $1.515^2/-10.8+1.47j/2.01+0.22j/1.33^2$ at a 632.8 nm wavelength light. The various lines in the two figures correspond to biomaterial films with thicknesses in the range of 6–18 nm per 3 nm. Specifically, the solid lines represent the *P* wave and the dashed lines represent the *S* wave. The solid lines in Fig. 2(a) clearly demonstrate the minimum reflectivity positions of the spectra, and in Fig. 2(b) show the phase jump in the SPR angle. Meanwhile, it is observed that the dashed lines representing the *S* wave remain virtually constant in both figures.

3 SPR Microarray and Imaging System

Molecular biologists conventionally utilize the method of hybridization, i.e., different sequences of probe DNA oligonucleotides with several tens to hundreds of nucleotides, which are complementary to the sequence of the labeled target DNA of interest. This approach is relatively time consuming because it is necessary to label the target DNA using some

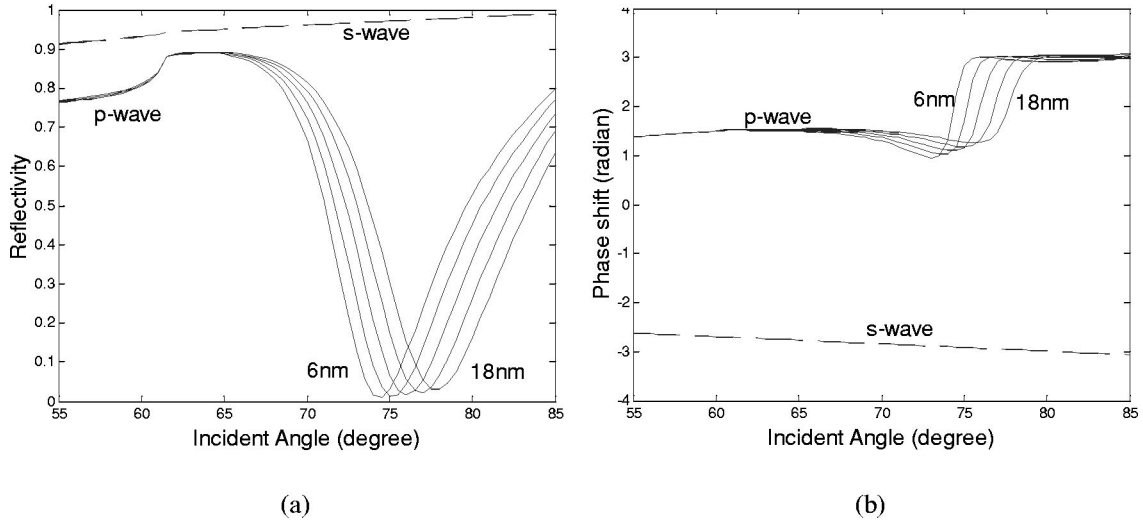

Fig. 2 Simulated curves of (a) the reflectivity and (b) the phase shift of the reflected light of a SPR sensor with a configuration of: BK7/Au film/biomaterial/water, with dielectric constants of $1.515^2/-10.8+1.47j/2.01+0.22j/1.33^2$, respectively. The thicknesses of the biomaterial films vary from 6 to 18 nm. The solid lines indicate the *P* wave and the dashed lines indicate the *S* wave.

form of fluorescent material. The major steps of the SPR biosensing technique employed to detect biomolecular interactions are first to immobilize the probe DNA or antibody on the SPR sensor, and then second to measure the change of the resonant condition in real time when the unlabeled target DNA or antigen interacts with the probe DNA or antibody. The biomolecular interaction can then be characterized and quantified, and the kinetic BIA performed.

3.1 *Design and Fabrication of SPR DNA Microarray*

To avoid chemical reaction with the metal film during the DNA immobilization process, it is preferable to select gold rather than silver as the film material. However, the poor adhesion of gold to glass presents difficulties, and hence a very thin chromium film (1–2 nm) is initially deposited on the glass as an underlay. In order to achieve optimum sensitivity, the deposited gold film must be of a thickness of 47.5 nm with 1 nm accuracy in accordance with Eq. (3) and its roughness must be controlled such that it is less than 10 Å root mean square. Array biosensing is employed to provide a high-throughput screening capability. In order to bind the probe DNA on the thin gold film slide, the slide is immersed in a 1 mM thiol solution $[HS(CH_2)_{15}COOH]$ for 6 h, and then placed in a solution with 1 mg/mL N-ethyl-N-(3-dimethylaminopropyl) carbodiimide hydrochloride (EDC hydrochloride, FLUKA, Switzerland) in 40 mM 2-(N-morpholino) ethanesulfonic acid (MES) for an additional 6 h. After cleaning the slide with de-ionized water and alcohol, the probe DNA is mechanically spotted in a matrix arrangement. Finally, a blocking solution (methanol) is applied to modify the functional group of thiol $-COOH$ into $-CH_3$ to prevent the target DNA from being captured on the free thiol/EDC area. Figure 3 presents a schematic illustration of the resulting SPR DNA microarray.

3.2 *SPR PSI Optical Setup*

Figure 4 presents the overall configuration of the proposed SPR-PSI imaging system. Initially, the incident angle of a single wavelength beam directed onto the SPR microarray is rotated in order to identify the angle at which the minimum reflectivity is obtained. This incident angle is then defined as the SPR angle of the imaging system. Subsequently, a collimated *P*-wave and *S*-wave light beam (typically He–Ne laser or laser diode generated) is directed through the prism at an incident angle close to the SPR angle in order to excite the slide with its deposited thin gold film and biomaterial. It is known that the SPW is excited only by the *P* wave at the SPR angle. Hence, the phase of the *P* wave is changed dramatically as a result of biomolecular interaction. Therefore, the *P* wave corresponds to the actual signal, and the *S* wave serves as a reference signal. The phase differences between the two waves, as measured by a modified Mach–Zehnder PSI system at various locations, create interference patterns, which are subsequently converted by using linear data analysis and Fresnel's calculations to analyze the biomolecular interaction. The modified Mach–Zehnder PSI system splits the reflected light from the SPR microarray into a corresponding *P* wave and *S* wave. Optical phase shifts are introduced into the *S* wave by means of a lead-zinc-titanate (PZT) transducer mirror and five sequential interferograms are then captured via a CCD camera.[19] The phase can then be reconstructed by means of the following equation and two-dimensional (2-D) phase unwrapping algorithms:

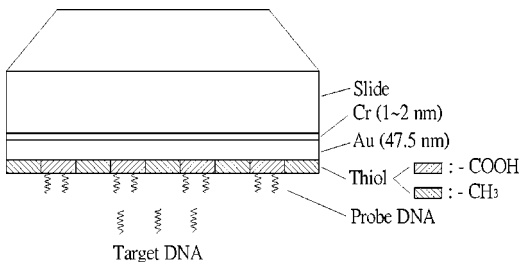

Fig. 3 SPR DNA microarray.

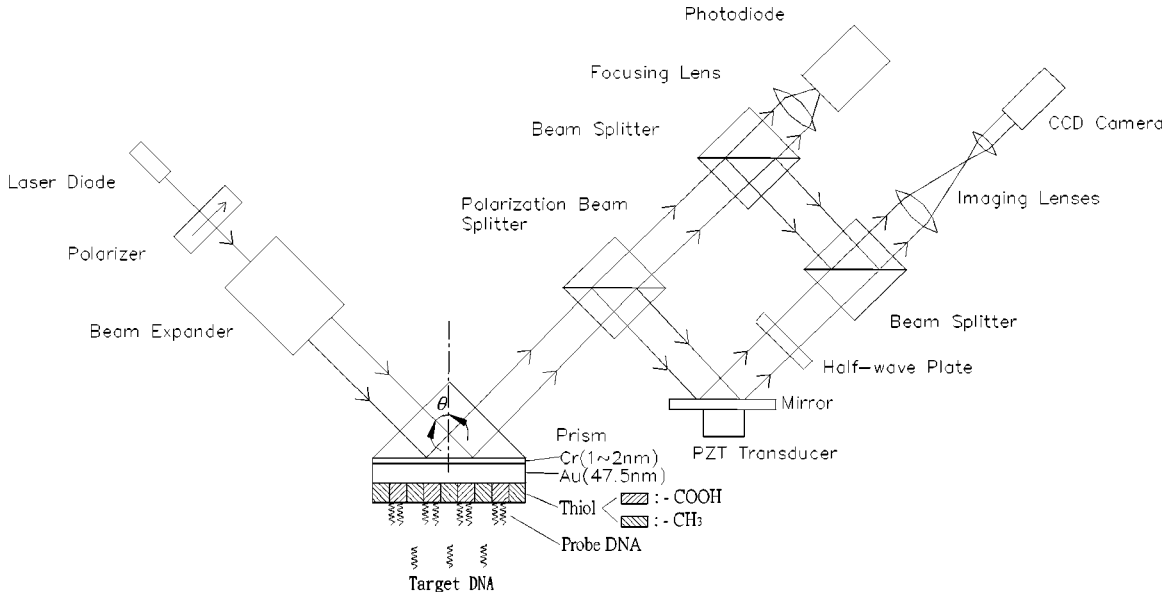

Fig. 4 Optical setup of SPR imaging system with Mach–Zehnder PSI for DNA microarray hybridization.

$$\phi(x,y)=\tan^{-1}\left[\frac{2(I_2-I_4)}{2I_3-I_5-I_1}\right], \tag{6}$$

where I_i is one of the five interferograms, $i=1,2,...,5$. Following the next subsection of phase reconstruction, 2-D measured phase data are established in terms of the biomolecular interaction and then converted to characterize the biomolecular interaction.

Five interferograms are recorded as the reference phase is systematically varied by the PZT transducer mirror. The wave front phase modulo 2π is then calculated at each measurement point as the arctangent of a function of the interferogram intensities measured at that individual spot. The current authors have previously developed a novel 2-D phase unwrapping method based on a multichannel least-mean-squares (MLMS) algorithm.[20] Compared to other phase unwrapping methods, this method not only provides noise immunity and a greater computational efficiency, but also demonstrates a noise-filtering capability.[21] The final wave front map is obtained by utilizing the MLMS unwrapping algorithm to remove the 2π phase discontinuities. A five-step reconstruction algorithm is used since it has a proven ability to overcome the uncertainty of the PZT.[19]

4 Experimental Results

This study performs two experiments to verify the resolution, accuracy, and stability of the proposed SPR-PSI imaging system. In the first experiment, the difference in refractive index Δn (1.5×10^{-5}) of N_2 and Ar are precisely determined to confirm the high global accuracy of the system, whereas in the second experiment, the high-throughput capability of the system is demonstrated for the DNA microarray.

4.1 *Global and Local Investigations*

The preliminary experiment confirms the feasibility of the SPR-PSI imaging system when the refractive indices of 100% N_2 and 100% Ar are significantly separated. Under controlled conditions, the difference in refractive index Δn is approximately 1.5×10^{-5}. During the experiment, the two gases entered the flow system at a flow rate of 50 mL/min through an extended temperature controlled chamber, which controlled the temperature variation to within 0.1 °C. Figure 5 shows the time dependence of the phase shift of the SPR-PSI imaging system during the sequential cyclic replacement of 100% N_2 with 100% Ar every 5 min. The phase difference between N_2 and Ar is measured to be 0.005π. After testing the short-term stability and long-term drift, it was found that the proposed SPR-PSI imaging system achieved a global resolution of better than $\pi/500$ with a 20×20 mm^2 detection area in the short term. Therefore, the global detection resolution corresponding to biomolecular interaction is of the order of 0.5 pg/mm^2 surface coverage. Additionally, the SPR-PSI imaging system

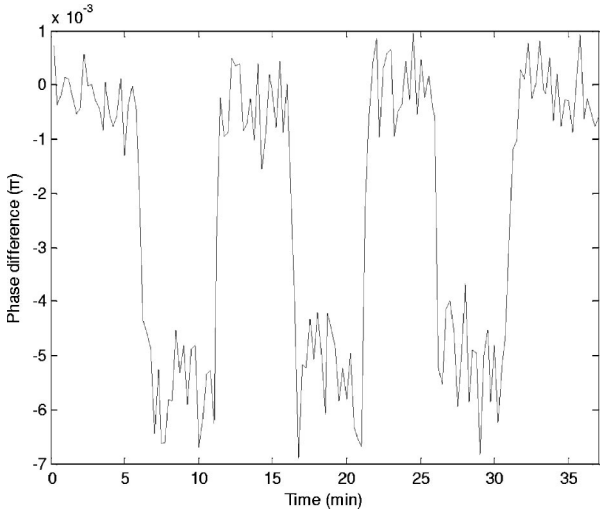

Fig. 5 Time-dependent phase change of interference fringes acquired by PSI techniques under cyclic replacement of 100% N_2 with 100% Ar.

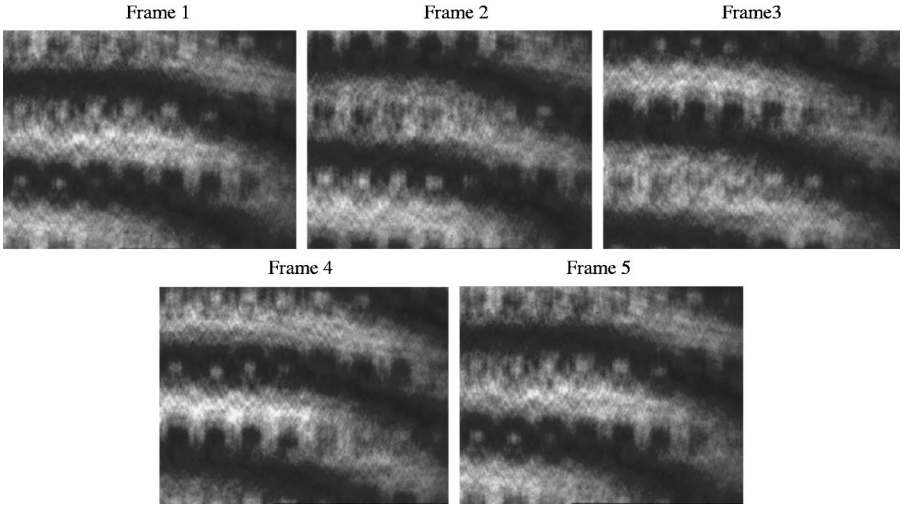

Fig. 6 Five interference frames for 32 thiol/ssDNA spots recorded by a CCD camera with 640×480 pixels.

demonstrated a detection limit of 2.5×10^{-7} refraction index change in the long-term phase stability of $\pi/100$ in 30 min, with a spatial phase resolution of $\pi/200$ with 100×100 μm^2 detection area. It is noted that the conventional SPR imaging system based on intensity variation measurements is incapable of detecting the tiny changes caused by the cyclic replacement of N_2 with Ar.

4.2 *Microarray Test*

A SPR DNA microarray was designed and fabricated in accordance with the procedure described previously in Sec. 3.1. A 1 μM 15-mer ssDNA (5′-GTTACCACACGGATG-3′) probe was mechanically spotted to form 320 individual spots within a 25×25 mm^2 area. The proposed system also enables simultaneous detection of DNA hybridization at all points of the SPR DNA microarray comprising more than one thousand different DNA spots if an automatic spotter is used to achieve an individual spot within a 100×100 μm^2 area. The completed SPR DNA microarray was then placed in contact with the coupled prism of the SPR-PSI imaging system using a matching oil. During the hybridization process, the target DNA hybridizes with the probe ssDNA if they are partially or completely complemental in the DNA sequence. The flow cell was controlled at a temperature of 35 °C to within 0.1 °C in order to reduce noise arising from the change of the dielectric constant of the gold film. In accordance with the procedure outlined in Sec. 3.2, the SPR angle of the SPR-PSI imaging system was identified from the intensity variation of the SPR reflectivity spectrum as the incident angle was rotated. The modified Mach–Zehnder interferometer was employed to record the interference pattern created by the phase differences between the *P* wave and the *S* wave. Where the target DNA hybridized with the spots of the probe ssDNA array, local variations were evident in these interference patterns. A PZT actuator was then employed to produce a sequential $\pi/2$ phase shift of the *S* wave, thereby creating an additional four interference frames. An accurate fringe analysis was then performed by means of the five-step phase reconstruction algorithm and the MLMS unwrapping algorithm.[19,20]

Figure 6 presents five interference frames for the 28 thiol/ssDNA spots in a 6×8 mm^2 area-scan CCD camera with 640×480 pixels. Each spot has a diameter of 0.5 mm and the distance between each probe ssDNA spot is 1 mm. If the sensing area includes a ssDNA spot, local variations of the interference pattern can be observed, as shown in Fig. 6. It is noted that frame 5 is created from frame 1 by incrementing the phase by $\pi/2$ four times consecutively. Therefore, frame 5 is similar to frame 1 since the 2π phase shift between them can be neglected. The phase difference is reconstructed using the five-step phase reconstruction algorithm, and then the biomolecular interaction is analyzed according to the phase difference by means of Fresnel's calculations. Figure 7(a) presents the reconstructed phase jump associated with six probe ssDNA spots. The phase difference between the areas with and without DNA is seen to be approximately 0.2π. The local resolution is $\pi/200$ with a 100×100 μm^2 detection area, i.e., the size of a probe DNA spot. Hence, by maintaining a detection resolution of approximately 1 pg/mm^2 surface coverage of the biomaterial, the screening area can simultaneously monitor up to 2500 individual spots in a 10×10 mm^2 area. Figure 7(b) shows the reconstructed phase variation in three different scanning lines, and clearly distinguishes between the locations of the screening area with and without the probe ssDNA. The results demonstrate that all spots of the SPR DNA microarray can be detected simultaneously in a single experiment and hence meets the requirements of DNA sequence diagnostics.

5 Conclusions

This study has presented a novel SPR-PSI imaging system for the analyses of DNA hybridization without the requirement for additional labeling. The SPR DNA microarray can simultaneously detect the target DNA, and hence meets the requirements of DNA sequence diagnostics in a single experiment. The experimental results have shown that the detection limit for each individual spot under the SPR-PSI imaging system is approximately 1 pg/mm^2. The developed SPR-PSI imaging system and its SPR DNA microarray can be employed to observe DNA microarray hybridization in real time, with high sensitivity, and at high-throughput screening rates. The fea-

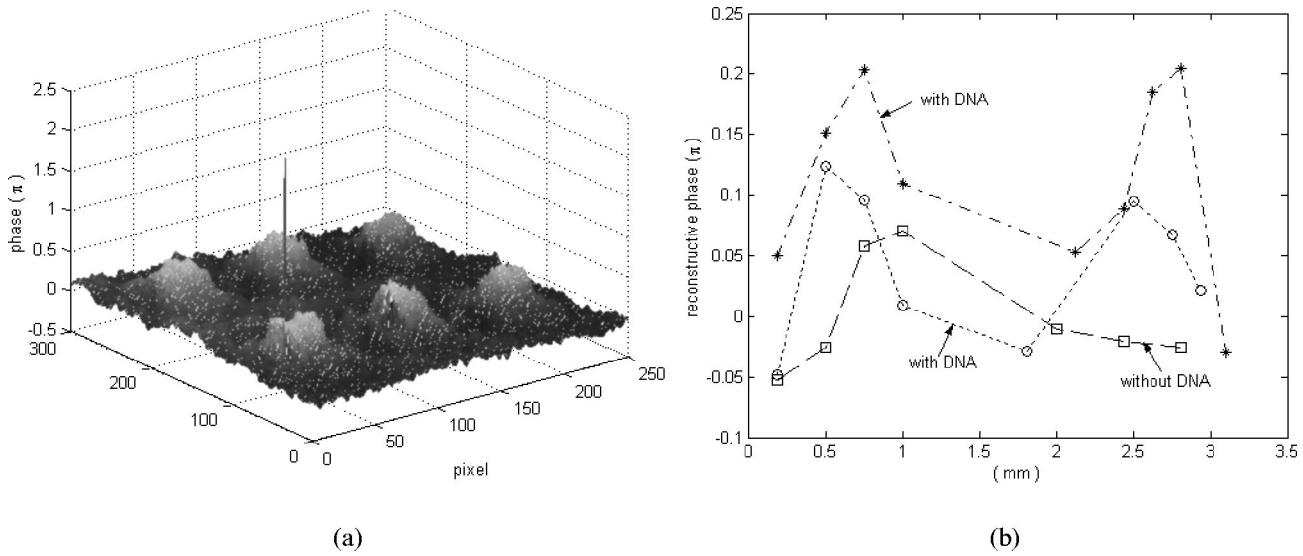

Fig. 7 SPR-PSI data analysis for 6 thiol/ssDNA spots. (a) Reconstructed phase shift between sensing area with and without probe ssDNA determined from five-step phase reconstruction algorithm and (b) reconstructed phase variation in three different scanning lines.

sible and swift measurement capabilities of the proposed SPR-PSI imaging system enable the device to be extended to the analysis of biomolecular interactions.

Acknowledgments

The authors gratefully acknowledge the support provided to this study by the National Science Council, Taiwan under Grant No. NSC 92-2215-E-006-024.

References

1. B. Liedberg, C. Nylander, and I. Lundsr, ''Surface plasmon resonance for gas detection and biosensing,'' *Sens. Actuators B* **4**, 299–304 (1983).
2. Z. Salamon, M. F. Brown, and G. Tollin, ''Surface plasmon resonance spectroscopy: probing molecular interactions within membranes,'' *Trends in Biomedical Sciences* **24**, 213–219 (1999).
3. G. Steiner, V. Sablinskas, A. Hubner, C. Kuhne, and R. Salzer, ''Surface plasmon resonance imaging of microstructured monolayer,'' *J. Mol. Struct.* **509**, 265–273 (1999).
4. H. Raether, *Surface Plasmons on Smooth and Rough Surfaces and on Gratings*, Springer, Berlin (1988).
5. S.-H. Kim, K.-S. Ock, J.-H. Im, J.-H. Kim, K.-N. Koh, and S.-W. Kang, ''Photoinduced refractive index change of self-assembled spiroxazaine monolayer based on surface plasmon resonance,'' *Dyes Pigm.* **46**, 55–62 (2000).
6. F. F. Bier, F. Kleinjung, and F. W. Scheller, ''Real-time measurement of nucleic-acid hybridization using evanescent-wave sensors: steps towards the genosensor,'' *Sens. Actuators B* **38**, 78–82 (1997).
7. E. Stenberg, B. Persson, H. Roos, and C. Urbaniczky, ''Quantitative determination of surface concentration of proteins with surface plasmon resonance using radiolabeled protein,'' *J. Colloid Interface Sci.* **143**, 513–526 (1991).
8. http://www.biacore.com/
9. C. E. Jordan and R. M. Corn, ''Surface plasmon resonance imaging measurement of electrostatic biopolymer adsorption onto chemically modified gold surface,'' *Anal. Chem.* **69**, 1449–1456 (1997).
10. http://www.htsbiosystems.com/
11. M. J. OBrien, V. H. Perez-Luna, S. R. J. Brueck, and G. P. Lopez, ''A surface plasmon resonance array biosensor based on spectroscopic imaging,'' *Biosens. Bioelectron.* **16**, 97–108 (2001).
12. B. P. Nelson, T. E. Grimsrud, M. R. Lies, R. M. Goodman, and R. Corn, ''Surface plasmon resonance imaging measurements of DNA and RNA hybridization adsorption on DNA microarrays,'' *Anal. Chem.* **73**, 1–7 (2001).
13. A. J. Haes and R. P. Van Duyne, ''A nanoscale optical biosensors: sensitivity and selectivity of an approach based on the localized surface plasmon resonance spectroscopy of triangular silver nanoparticles,'' *J. Am. Chem. Soc.* **124**, 10596–10604 (2002).
14. P. Englebienne, A. Van Hoonacker, and M. Verhas, ''High-throughput screening using surface plasmon resonance effect of colloidal gold nanoparticles,'' *Analyst (Cambridge, U.K.)* **126**, 1645–1651 (2001).
15. A. V. Kabashin and P. I. Nikitin, ''Surface plasmon resonance interferometer for bio- and chemical-sensors,'' *Opt. Commun.* **50**, 5–8 (1998).
16. P. I. Nikitin, A. N. Grigorenko, A. A. Beloglazov, M. V. Valeiko, A. I. Savchuk, O. A. Savchuk, G. Steiner, C. Kuhne, A. Huebner, and R. Salzer, ''Surface plasmon resonance interferometry for micro-array biosensing,'' *Sens. Actuators, A* **85**, 189–193 (2000).
17. A. G. Notcovich, V. Zhuk, and S. G. Lipson, ''Surface plasmon resonance phase imaging,'' *Appl. Phys. Lett.* **76**, 1665–1667 (2000).
18. F.-M. Hsiu, S.-J. Chen, C.-H. Tsai, C.-Y. Tsou, Y.-D. Su, G.-Y. Lin, K.-T. Huang, J.-J. Chyou, W.-C. Ku, S.-K. Chiu, and C.-M. Tzeng, ''Surface plasmon resonance imaging system with Mach-Zehnder phase-shift interferometry for DNA micro-array hybridization,'' *Proc. SPIE* **4819**, 167–174 (2002).
19. P. Hariharan, B. F. Oreb, and T. Eiju, ''Digital phase-shifting interferometry: a simple error-compensating phase calculation algorithm,'' *Appl. Opt.* **26**, 2504–2505 (1987).
20. J.-J. Chyou, S.-J. Chen, and Y.-K. Chen, ''Two-dimensional phase unwrapping using a multichannel least-mean-square algorithm,'' *Appl. Opt.* **43**, 5655–5661 (2004).
21. D. G. Ghiglia, G. A. Mastin, and L. A. Romero, ''Cellular-automata method for phase unwrapping,'' *J. Opt. Soc. Am. A* **4**, 267–280 (1987).